

Article

Future Scenarios of Bioclimatic Viticulture Indices in the Eastern Mediterranean: Insights into Sustainable Vineyard Management in a Changing Climate

Karam Alsafadi ^{1,2}, Shuoben Bi ^{2,*}, Bashar Bashir ³, Abdullah Alsaman ³ and Amit Kumar Srivastava ⁴

¹ School of Environmental Science and Engineering, Nanjing University of Information Science and Technology, Nanjing 210044, China

² School of Geographical Sciences, Nanjing University of Information Science and Technology, Nanjing 210044, China

³ Department of Civil Engineering, College of Engineering, King Saud University, P.O. Box 800, Riyadh 11421, Saudi Arabia

⁴ Institute of Crop Science and Resource Conservation, University of Bonn, 53111 Bonn, Germany

* Correspondence: bishuoben@163.com

Abstract: The evaluation of bioclimatic viticulture indices (BVIs) zones, similar to any other crop, necessitates a comprehensive understanding of the spatial variability of climate data. This study focuses on assessing the suitability of BVIs in the Jabal Al Arab region, a significant viticulture area in the Eastern Mediterranean. The aim is to analyze four temperature-based bioclimatic indices and the hydrothermal coefficient (HTC) to map their patterns and spatial variation across the region under climate change scenarios. Daily temperature data from 15 meteorological stations and 57 rain gauges spanning 1984–2014 were utilized, along with downscaled future scenarios (the Representative Concentration Pathways (RCPs) based on the second generation Canadian Earth System Model (CanESM2)) for 2016–2100. Additionally, statistical analysis and hybrid interpolation (regression-kriging) were employed to accurately map the BVIs throughout the region. The results reveal substantial spatial variability in Jabal Al Arab's climate, with heat accumulation and the hydrothermal index during the growing season significantly influenced by elevation and distance to the seacoast. Additionally, the viticulture zones vary based on the specific index used and the projected future climate scenarios compared to the current climate. Climate change projections indicate a trend toward warmer conditions in the future. Under the RCP scenarios, the region can be categorized into up to three bioclimatic classes for certain indices, in contrast to the current climate with six classes. These findings offer valuable insights into viticulture suitability within each climatic region and facilitate the identification of homogeneous zones. By employing consistent bioclimatic indices and advanced hybrid interpolation techniques, this study enables meaningful comparisons of Jabal Al Arab with other viticulture regions worldwide. Such information is crucial for selecting suitable grapevine varieties and assessing the potential for grape production in the future.

Keywords: grapevine (*Vitis vinifera*); hybrid interpolation; climate change; CanESM2; agro-climatic indices; sustainable farming; regression-kriging; RCPs; Syria



Citation: Alsafadi, K.; Bi, S.; Bashir, B.; Alsaman, A.; Srivastava, A.K. Future Scenarios of Bioclimatic Viticulture Indices in the Eastern Mediterranean: Insights into Sustainable Vineyard Management in a Changing Climate. *Sustainability* **2023**, *15*, 11740. <https://doi.org/10.3390/su151511740>

Academic Editor: Hossein Azadi

Received: 26 June 2023

Revised: 27 July 2023

Accepted: 28 July 2023

Published: 30 July 2023



Copyright: © 2023 by the authors. Licensee MDPI, Basel, Switzerland. This article is an open access article distributed under the terms and conditions of the Creative Commons Attribution (CC BY) license (<https://creativecommons.org/licenses/by/4.0/>).

1. Introduction

Grapevine (*Vitis vinifera*) holds significant cultural, ecological, and economic importance in the Mediterranean Basin, making it a major crop with the largest acreage among fruit products [1,2]. The production of grapevines is influenced by various interconnected environmental conditions [3], often encompassed by the term “terroir.” While there is ongoing debate regarding its precise definition, most definitions attempt to capture the combination of micro-climatic factors, soil characteristics, topography, geology, and their intricate interrelationships [4–6]. The International Organization of Vine and Wine (OIV)

has defined “terroir” as having a geographical dimension, emphasizing the necessity for zoning and delimitation, particularly with regard to agroecological factors such as climate and soil [7]. However, in research aimed at determining the suitability of specific sites for vineyards or the cultivation of particular grapevine varieties, the influence of meteorological elements in the delimitation of zones should carry more weight than soil characteristics [3,7].

Since temperature variability can significantly impact viticultural areas at different scales, various temperature-based bioclimatic viticulture indices (BVIs) have been developed. These include the Winkler Index (WI-GDD) [8], the Huglin Index [9], the cool night index (CI) [10], and the hydrothermal coefficient (HTC), which integrates the effects of temperature and precipitation during the growing season [11]. BVIs have been extensively studied in viticultural regions worldwide using diverse approaches. Examples include Argentina [12,13], Australia [14,15], Europe [16], New Zealand [17], Croatia [18], central Chile [19], the western USA [20], Hungary [21], Serbia [22], Romania [23], the province of Quebec in Canada [24], the State of Washington and parts of northeast Oregon in the USA [25], and even globally [10]. Smaller regions such as the Miño river valley in Spain [26], Turkey’s Black Sea region [27], the Portuguese Douro valley region [28,29], the western slopes of Jabal Al Arab in Syria [3], the Apulian region in Italy [30,31], and Santorini Island in Greece [32] have also been studied.

As part of the Eastern Mediterranean region, the agricultural sector in southern Syria faces significant challenges related to various environmental issues. These challenges include soil erosion [33], the impact of climate change on agricultural production [34], and the negative consequences of unsustainable agricultural practices on soil health [35]. Among the agricultural activities in this region, viticulture holds great importance as it supports the livelihood of the local population and contributes to food industries such as grape wines, molasses, and raisins. However, similar to other agricultural sectors, viticulture also encounters several environmental problems, including unsustainable management practices [3] and difficulties associated with the availability of soil micronutrients for vineyard cultivation [36]. Research conducted by Mohammed et al. [36] revealed that the majority of studied soils in southern Syria, specifically for vineyard cultivation, exhibit micronutrient concentrations below the critical level. To promote sustainable viticulture practices, Al-safadi et al. [3] developed new maps that analyze optimal regions for economically viable viticulture production in this area. These maps incorporate climate-viticulture indices, soil requirements, and other topographic indicators to identify suitable locations for cultivating vineyards. These maps aim to assist decision-making processes in selecting new cultivation sites and support the development of sustainable viticulture practices in the region.

To enhance the management of local viticultural regions in response to global warming and climate change, it is crucial to have high-resolution data that accurately depict the spatial distribution BVIs [37–39]. General circulation models (GCM) of climate change often lack the precision required to delineate the variability of BVIs at the local level, which typically operates at approximately 100–300 km spatial resolution. Additionally, the calculation of BVIs often relies on a small number of locations connected through climatic station sites or coarse-resolution distributed datasets. Consequently, the methods employed to precisely delineate symmetrical regions may not generate accurate maps. Several algorithms and methods have been employed to generate fine-scale gridded data for BVIs. These include geostatistical approaches [40], dynamical and statistical downscaling [41,42], and dynamical and geostatistical techniques [43]. Remote-sensing-based modeling utilizing MODIS-land surface temperature (LST) has been utilized [44], along with downscaling of MODIS-LST through machine learning regression models [45] and statistical methods such as multivariate linear regression and non-linear support vector regression [39]. Other methods employed include the regression-kriging (RK) method [46] and the Weather Research and Forecasting model WRF [38]. In general, hybrid interpolation algorithms are preferred, particularly when incorporating auxiliary information and interpolating the models’ residuals. Numerous studies have indicated that the RK technique is suitable for

this purpose [30,46–48]. By utilizing these advanced methods, it becomes possible to generate accurate and detailed maps of BVIs, enabling better understanding and management of viticultural regions in the face of climate change.

Our study focuses on the mapping of precipitation- and temperature-based BVIs at a fine resolution during the growing seasons in the prominent viticulture regions of Jabal Al Arab, situated in the Eastern Mediterranean. The mapping covers the period from 1984 to 2014 and incorporates downscaled climate change scenarios based on the second generation Canadian Earth System Model (CanESM2) and three Representative Concentration Pathways (RCPs) from 2015 to 2100. To achieve this, we employed the regression-kriging (RK) model, allowing us to generate maps at a high resolution of 1000 m intervals. For the implementation of the RK model, we utilized daily observed temperatures and applied the regression method. To enhance the accuracy of the model, we conducted a regression analysis of BVIs using a range of terrain characteristics obtained from a Digital Elevation Model (DEM) and auxiliary information. This approach has been successfully employed in previous studies and demonstrated superior performance compared to a simple regression model. By utilizing the RK model and incorporating various terrain characteristics and auxiliary information, we aim to produce highly detailed maps of BVIs, providing valuable insights into the viticulture regions of Jabal Al Arab. Additionally, we extended our analysis to include climate change projections based on the CanESM2 model and RCPs, enabling us to assess the potential impacts of future climate scenarios on viticulture in the region.

2. Materials and Methods

2.1. Study Area, Data Collection, and Preliminary Analysis

The study area under investigation is situated in the Eastern Mediterranean, specifically in southwestern Syria and northern Jordan. Geographically, it lies between latitudes 32°18' N and 33°13' N, and longitudes 36°20' E and 37°02' E, encompassing an area of 3458 km² (Figure 1a). The climate in this region is characterized as continental, with cold and wet winters, and hot and dry summers. In July, average temperatures during the summer range between 18 °C and 32 °C, while in January, winter temperatures average between 3 °C and 10 °C (Figure 1b). The average annual precipitation in the region is 350 mm, with the maximum recorded rainfall being approximately 570 mm in the elevated area (Figure 1a). The majority of rainfall is concentrated in the winter season, with the mean monthly precipitation in February ranging from 10 mm to 145 mm. Based on the Köppen–Geiger classification, the central and western hilly regions of the study area fall within the temperate wet climatic zone, whereas the eastern part is characterized by a desert (arid) or semi-arid (continental or steppe) climate. The altitudes in the region vary from 696 m in the western part to 1795 m above sea level in the central part (Tall Qeni). The area holds significant importance as a viticulture region in the Eastern Mediterranean, with a total viticultural area of approximately 10,125 ha in 2015. According to the Syrian Ministry of Agriculture and Agrarian Reform (SMOAR), the region is the second most important in terms of viticulture, following apples. Vineyards are a crucial source of income for thousands of families, with an annual production of no less than 40,000 tons. The cultivation of vineyards in this region is deeply rooted in the region's economic heritage, passed down from previous generations.

In this study, the modeling of the BVIs gridded data at a fine spatial resolution of the study area was based on in situ data from several sources, which can be explained as follows:

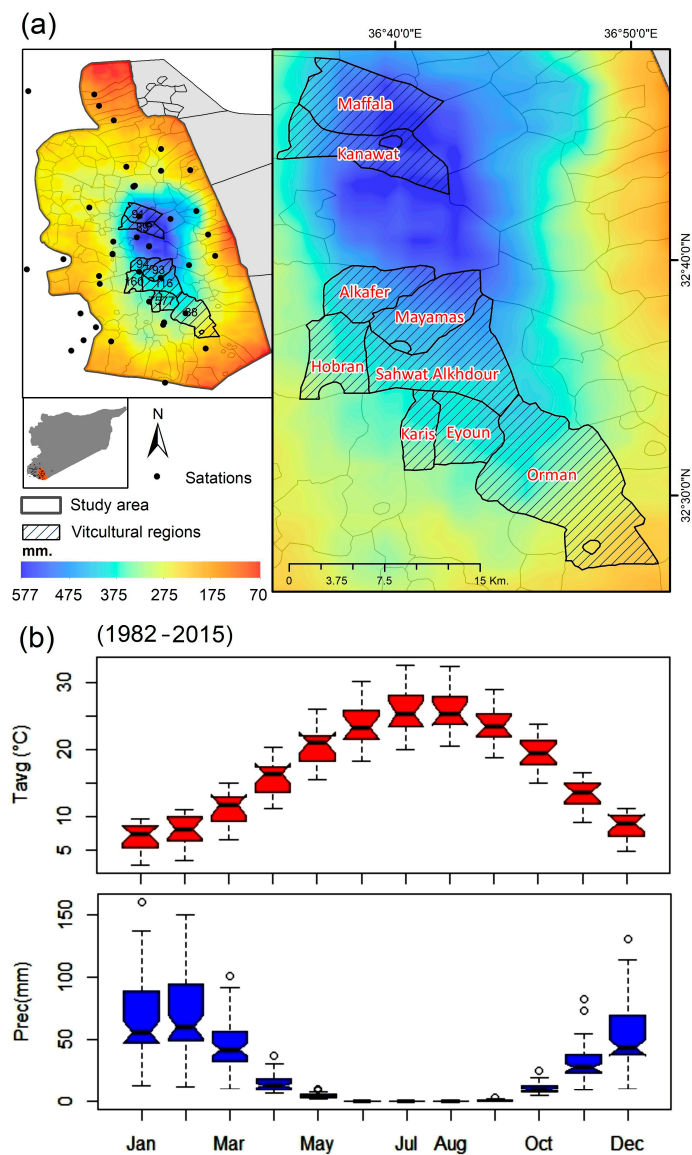


Figure 1. (a) Study area, spatial distribution of stations location, annual precipitation (mm) [48], and studied viticultural regions, (b) seasonal cycles of temperature and precipitation in the study area.

2.1.1. Observed Air Temperature and Precipitation

To fulfill the main objectives of our research, we utilized in situ data obtained from various sources, including 57 rain gauges and 15 climatic stations. These data were sourced from the Syrian Meteorological Authority (SMA), SMOAAR, and the Jordan Meteorological Department (JMD) database. The selection of stations took into consideration their location, both within and outside the study area, as depicted in Table 1. Daily data spanning from 1984 to 2014 were collected for analysis. During the data preparation phase, we included stations with observations covering a minimum of 20 years to ensure data reliability. To address any missing values and ensure uninterrupted data acquisition, gap-filling techniques were applied. Specifically, we utilized 7 rain gauges with complete data and 9 gridded points of temperature variables from the NASA Power Data, which have a resolution of 0.5° arc degree, as reference data for correction, gap filling, and homogeneity testing. Regardless of the spatial interpolation method employed, careful data preparation and handling were necessary. This involved removing outliers, selecting candidates and reference stations, filling data gaps, and conducting homogeneity tests. It is important to note that when dealing with data from multiple sources, each with its own settings, these steps are crucial

to obtain high-quality data for reliable climate assessment. To ensure data quality, a rigorous procedure was implemented, which included analyzing the difference series between candidate stations and their neighboring stations through pairwise comparisons. Missing values were interpolated using simple linear regression. Furthermore, the Standard Normal Homogeneity Test (SNHT), as proposed by Alexandersson [49], was applied to assess data homogeneity. For detailed information on the quality control and homogeneity testing process, refer to the attached documentation for the AnClim software [50].

Table 1. Observed data used in this study.

Variable	Data Type	Number of Station/Point	Temporal Scale	Reference Period	Source
Precipitation (mm)	Rain gauge and climatic stations	57	Monthly Daily	1984–2014	SMA, SMOAAR, and JMD
Temperature (°C)	Climatic stations	15	Daily	1984–2014	SMA, SMOAAR, and JMD
Temperature (°C)	Gridded data	9	Daily	1984–2014	NASA Power Data release 8.0.1 https://power.larc.nasa.gov (Accessed on 15 February 2023)

2.1.2. CIMP5 Climate Projection (CanESM2)

The large-scale standardized climatic variables of CanESM2 and the NCEP (National Centers for Environmental Prediction) reanalysis dataset were used to assess the current climate and projected climate change under the RCPs. These datasets are available from the Canadian Climate Data and Scenarios website (<http://climate-scenarios.canada.ca>, (accessed on 15 February 2023)) for the baseline climate period of 1961–2005 and future scenarios from 2006–2100 under three RCPs (RCP2.6, RCP4.5, and RCP8.5). The spatial resolution of the data is approximately 2.81 degrees, with longitude and latitude values relatively fixed. To represent nearly observed station data in the study area, the “BOX_014X_44Y” grid cell from CanESM2 was selected. However, due to the coarse spatial resolution of general circulation models (GCMs), their applicability in impact evaluation research, environmental planning, adaptation, and decision making at regional and local scales is limited. Furthermore, uncertainties and biases associated with GCMs increase when compared to regional and local scales, further limiting their usefulness in local-scale assessments and environmental planning studies. To address this, a downscaling process was employed to increase spatial resolution, reduce potential biases, and provide finer spatial information. The Statistical DownScaling Model (SDSM) [51] was adopted to downscale the outputs from CanESM2. This method involves statistically fitting a relationship between local-scale climatic variables (predictands) and large-scale climatic variables (predictors) using a multiple regression model and bias correction methods [52,53]. In this study, the SDSM software was used to downscale the CanESM2 outputs. The observed monthly precipitation data from 57 rain gauges and average, maximum, and minimum temperatures from 15 synoptic weather stations were utilized. Additionally, 26 predictors from the NCEP reanalysis data and CanESM2 (see Table 1 in Gebrechorkos et al. [54] study) were imported into the software for model fitting, validation, and future projections.

2.2. Bioclimatic Viticulture Indices (BVIs)

Five BVIs were calculated to assess the impact of climate change on viticulture in the Eastern Mediterranean:

- (i) The hydrothermal coefficient (HTC) was introduced by Branas et al. [11] as a measure that combines the influence of seasonal precipitation and temperature specifically during the growing season. Its purpose is to assess water availability for vineyards and determine the suitability of rainfed viticulture [55]. In areas where HTC values fall below 0.5 mm/°C, grape production can only be sustained with high air humidity or irrigation. The HTC ranges from 1.5 to 2.5 mm/°C, with an optimal value of 1.0 mm/°C [55].

$$HTC = \frac{10P}{GDD} \quad (1)$$

P represents the rainfall during the growing season in millimeters, and GDD denotes the cumulative effective degree days above 10 °C.

- (ii) The Winkler Index (WI-GDD) is commonly used to estimate the heat accumulation during the growing season for vineyards. Traditionally, this index calculates the total daily average temperatures from April to the end of October, using a base temperature of 10 °C, as proposed by Amerine and Winkler [8]. In our study, due to the warm climate in the region compared to higher altitude areas, we extended the calculation period from March to the end of September. The WI-GDD can be expressed as follows:

$$GDD = \begin{cases} \sum_{Mar\ 1st}^{Sept\ 30th} (T_{avg} - 10); & T_{avg} \geq 10 \\ 0; & T_{avg} < 10 \end{cases} \quad (2)$$

$$T_{avg} = \left(\frac{T_{max} + T_{min}}{2} \right) \quad (3)$$

- (iii) The Huglin Index (HI) was developed by Huglin [9] and is calculated similarly to the WI-GDD, but with a greater emphasis on maximum temperature and an adjustment based on latitude, specifically the length of the day coefficient [9]. The HI provides more detailed information on the sugar potential of specific grape varieties and offers qualitative insights when combined with the values of the CI cool night index [10]. Jones et al. [56] and Hall and Jones [14] have updated the HI formula to accommodate all latitudes, considering the months from April to September in the Northern Hemisphere and excluding October, as they believe that the values become less significant during the harvest period [17,20]. In this study, we began accumulating daily average temperatures from March, using a coefficient length of the day of “d = 1”.

$$\sum_{Mar\ 1st}^{Sept\ 30th} \left(\frac{(T_{avg} - 10) + (T_{max} - 10)}{2} \right) d; T_{avg} \geq 10 \quad (4)$$

$$T_{avg} = \left(\frac{T_{max} + T_{min}}{2} \right) \quad (5)$$

- (iv) The cool night index (CI) was developed by Tonietto and Carbonneau [10] to assess the degree of coolness during nighttime by considering the average minimum temperatures in the ripening month, typically September in the Northern Hemisphere. This climatic factor significantly influences grape and wine characteristics, including color and aromas. The CI is particularly useful for evaluating the qualitative aspects of wine grapes, specifically the presence of secondary metabolites such as aromas and polyphenols in grape juice [57]. To calculate CI, the minimum air temperatures in September are averaged and expressed in degrees Celsius for the Northern Hemisphere. In the Southern Hemisphere, the calculation involves averaging the minimum air temperatures in March, also expressed in degrees Celsius [10]. These climate-viticulture indices, which also include the previously mentioned ones, enable the assessment of the optimal climatic suitability in terms of heat, water availability, phenological development throughout the growing season, and ripening conditions [58]. See Table 2 for more details regarding the climate-viticulture indices zones.

Table 2. The applied BVIs in this study and their class interval.

BVIs	Unit	Class of BVIs, and Class Interval	Reference
Growing season temperatures (GST)	°C	Cool (C)	13–15
		Temperate (T)	15–17
		Warm (W)	17–19
		Hot (H)	19–24
Hydrothermal coefficient (HTC)	–	Excessively dry (ED)	<0.25
		Dry (D)	0.25–0.5
		Moderately dry (MD)	0.5–1.5
		Moderately wet (MW)	1.5–2
		Wet (W)	2–2.5
Winkler Index growing degree days (WI-GDD)	GDD	Excessively wet (EW)	>2.5
		Too cold (TC)	<850
		Cold (C)	850–1390
		Moderately cold (MC)	1391–1670
		Warm (W)	1671–1940
		Moderately warm (MW)	1941–2220
Huglin Heliothermal index (HI)	GDD	Hot (H)	2221–2700
		Too hot (TH)	>2700
		Too cold (TC)	<1200
		Very cool (VC)	1200–1500
		Cool (C)	1500–1800
		Temperate (T)	1800–2100
		Temperate warm (TW)	2100–2400
		Warm (W)	2400–2700
Cool night index (CI)	°C	Very warm (VW)	2700–3000
		Too hot	>3000
		Too cold (TC)	<1200
		Very cool nights (VCN)	<12
		Cool nights (CN)	>12 ≤ 14
		Temperate nights (TN)	>14 ≤ 18
		Warm nights (WN)	>18

- (v) The growing season temperatures (GST) is a climate-maturity zoning system created by Jones [59] to classify regions based on the correlation between phenological needs and growing season temperatures. It encompasses a range of climates, from cool to hot, to cultivate high-quality grapevines in globally recognized regions and for commonly grown grape varieties. The GST system assists in identifying the favorable climate conditions required for optimal grapevine growth and maturity during the growing season.

2.3. Fine-Scale Modeling of BVIs Using Regression-Kriging (RK)

To accurately produce regional zones of BVIs at a fine spatial resolution, it is necessary to obtain BVIs for each pixel with fixed horizontal spacing grids, taking into consideration the environmental lapse rate. The environmental lapse rate represents the ratio of BVIs' change with variation in altitude, which leads to variations in temperature accumulation during the growing season due to complex terrains. Typically, these procedures involve using a Digital Elevation Model (DEM) and employing local regression equations and hybrid interpolation methods such as regression-kriging [30,46,47]. Geostatistical interpolation approaches recognize that the geographical variation in any continuous variable, including each BVI, is often too irregular to be described by a simple mathematical function. Instead, a stochastic surface can better explain the variation. The regression-kriging (RK) method [60,61] is applied, where each BVI is independently determined using the multivariate regression trend (MR), and the MR's residuals are added back in the next step. This

process allows the obtaining of BVIs with fixed horizontal spacing grids at each unsampled pixel x based on the following equation:

$$Z_{RK}(x) = MR(s) + RS(s) \quad (6)$$

where the regressions, $MR(s)$, are fitted by the MR, and the MR's residuals, $RS(s)$, are predicted using the ordinary kriging (OK) method. The predictions were expressed in the equation:

In Equation (6), $Z_{RK}(x)$ represents the predicted value of the BVIs at unsampled pixel x . It is obtained by adding the regressions, $MR(s)$, fitted by the multivariate regression trend (MR), with the predicted residuals, $RS(s)$, using the OK method. The predictions are expressed as follows:

$$Z_{RK}(x) = \sum_{j=0}^p \beta_j(s_0) \times v_j(s_0) + \sum_{i=1}^n \omega_i \times RS(s_i) \quad (7)$$

Z_{RK} represents the estimation at a specific site (x), $\beta_j(s_0)$ are the unstandardized coefficients of the MR, $v_j(s_0)$ is the predictor (value of the independent variable) at the same site. p is the number of predictors used in RM models, ω_i is the weight fixed by applying the OK method of the MR residuals, $RS(s_i)$, for n neighboring observed points.

In Equation (7), Z_{RK} represents the estimation at a specific site (x). The equation is comprised of two main parts. The first part is the sum of the products of unstandardized coefficients, $\beta_j(s_0)$, and predictors, $v_j(s_0)$, at the same site. This represents the contribution of the multivariate regression trend (MR) to the estimation. The sum is performed over all p predictors used in the MR models. The second part is the sum of the products of weights, ω_i , and the predicted residuals, $RS(s_i)$, obtained from applying the OK method to the MR residuals. This represents the contribution of the spatial interpolation of the residuals to the estimation. The sum is performed over n neighboring observed points. Together, these two parts combine to provide the estimation Z_{RK} at the specific site x .

To achieve this, the elevation data for the study area was obtained by calculating and extracting it from the Digital Elevation Model (DEM) provided by the U.S. Geological Survey's Center for Earth Resources Observation and Science (EROS) Archive—Digital Elevation—Global (GTOPO30) within the HYDRO1k project data [62]. The DEM had a horizontal grid spacing of 30 arc-seconds, which corresponds to approximately 1 km resolution. Geographic data such as longitudes, latitudes, and distances to the sea coastline were also collected. Additionally, MODIS cloud cover data were acquired for the study area, which was used for precipitation modeling [47]. These data, along with the elevation data, were utilized in fitting the multivariate regression (MR) models using the principal component method. This approach helped address the issue of multicollinearity that can arise when using correlated variables in the MR method. It should be noted that the RK method, which was employed for spatial interpolation, tends to provide more accurate predictions when the variables are available at all locations within the region. In this study, regular gridded data at a resolution of 1000 m were used to obtain the BVIs for the entire study area, while station-based BVIs estimates were obtained for a fixed horizontal spacing grid, resulting in a continuous surface. This approach allowed for the determination of BVIs values for each smallest resolution unit (pixel) within the study area. Four raster BVI models were created: one representing the current climate for the period of 1984–2014, and three models for different climate change scenarios (Representative Concentration Pathways—RCPs). All of the procedures described above were carried out using the geostatistical tool package within the ArcGIS 10.8 environment (Esri, Redlands, CA, USA).

3. Results

3.1. Projected Change in Temperatures and Precipitation

Estimates were conducted to assess the spatiotemporal variability of mean air temperature and annual precipitation anomalies under the CanESM2 projection for the period 2015–2100, considering three RCPs—RCP2.6, RCP4.5, and RCP8.5. The baseline period used for comparison was 1984–2014, and the analysis was carried out across 15 stations in southern Syria. The results reveal that under RCP2.6, the average anomalies in mean air temperature across all 15 stations were 1.73 °C. The highest average temperature anomaly was recorded in August (2.42 °C), while the lowest was observed in November (0.83 °C). These findings indicate that the average air temperature was higher than the baseline values across all stations. Similar patterns were observed for RCP4.5 and RCP8.5, with average anomalies of 2.13 °C and 3.16 °C, respectively, across all months. The highest average anomalies occurred in February and March, with values of 4.14 °C and 4.1 °C for RCP4.5, and in August and September, with values of 3.65 °C and 3.75 °C for RCP8.5. On the other hand, the lowest anomalies were observed in October, with a value of -1.25 °C for RCP4.5, and in April, with a value of 2.35 °C for RCP8.5. However, under RCP4.5, the anomalies in mean air temperature were negative in October and November across all regions, indicating that the temperature during these months became colder compared to the baseline values (Figure 2).

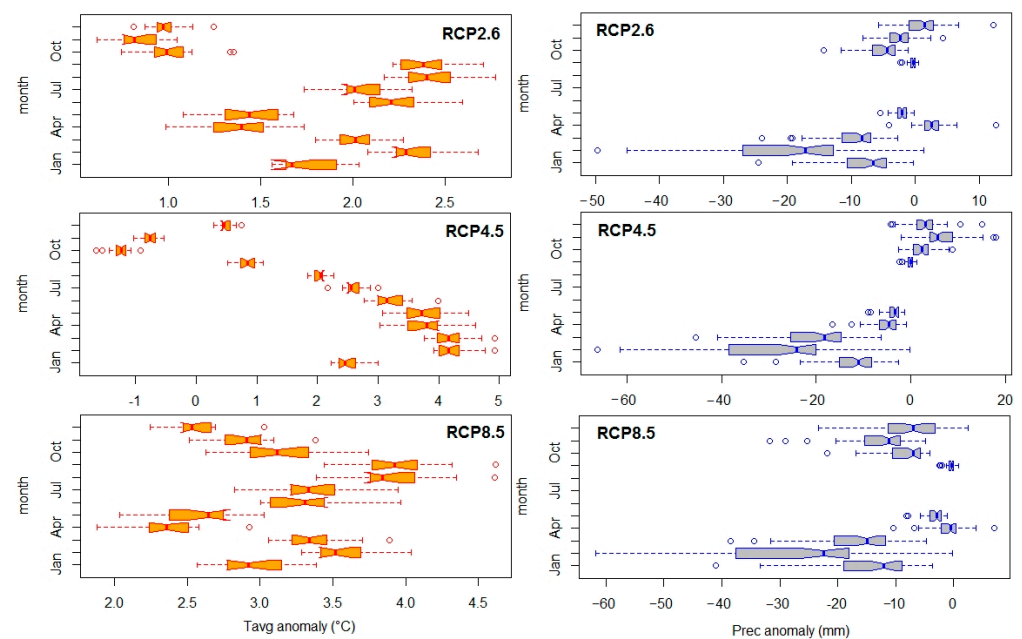


Figure 2. Spatial-temporal change in monthly precipitation and temperature using CanESM2 future scenarios spanning from 2015 to 2100 under the RCPs in comparison to the baseline period of 1984–2014.

Regarding precipitation, across 57 stations in southern Syria, the estimated reduction in cumulative monthly precipitation compared to baseline values was 44.6 mm, 59.4 mm, and 91.5 mm under RCP2.6, RCP4.5, and RCP8.5, respectively. The stations of Ain Arab and Al Tanf exhibited the highest and lowest reductions in precipitation amounts across the different RCPs. Under RCP2.6, the maximum reduction was 120.9 mm (Ain Arab) and the minimum reduction was 14.0 mm (Al Tanf). Similarly, under RCP4.5, the maximum reduction was 150.9 mm (Ain Arab), and the minimum reduction was 19.3 mm (Al Tanf), while under RCP8.5, the maximum reduction was 231.7 mm (Ain Arab), and the minimum reduction was 25.7 mm (Al Tanf). Furthermore, under RCP4.5, the anomalies in monthly precipitation were positive in October, November, and December across all regions, indi-

cating that the precipitation during these months became wetter compared to the baseline values (Figure 2).

3.2. Current Temporal Trends and Projected Change in BVIs

Estimates of the BVIs were conducted for three regions, namely Ain Arab, Kafer, and Orman, for a baseline period of 31 years from 1984 to 2014. Figure 3 shows the temporal evolution of HI and WI-GDD values during the period 1984–2014 for the Kafer and Orman regions, indicating a tendency of increase (statistically significant, $p < 0.05$), as well as for the three RCPs—RCP2.6, RCP4.5, and RCP8.5—over 86 years from 2015 to 2100 (Figure 4). The study found that the highest increase in WI-GDD under RCP2.6 compared to the baseline was estimated in Orman (18.5%), followed by Kafer (17.6%) and Ain Arab (6.6%). This same trend was observed under RCP4.5 and RCP8.5 in all three regions, with the highest magnitudes being 29.5%, 28%, and 16.1% under RCP4.5, and 35.8%, 33.6%, and 22.9% under RCP8.5, respectively (Table 3 and Figure 4). In addition, the coefficient of variation (CV) varied across the three regions and different scenarios, with the lowest CV being 3.8% under RCP2.6 in Ain Arab and the highest being 16.9% under RCP8.5, also in Ain Arab. For Al Kafer, the CV ranged from 3.0% under RCP2.6 to 12.7% under RCP8.5, while for Orman, it ranged from 3.3% under RCP2.6 to 14.3% under RCP8.5. Regarding the change in HI, the study estimated that the highest increase under RCP2.6 compared to the baseline was in Orman (16.2%), followed by Kafer (14.3%) and Ain Arab (5.9%). This same trend was observed under RCP4.5 and RCP8.5, with magnitudes of 25.9%, 22.5%, and 15.8% under RCP4.5, and 30.8%, 26.6%, and 21.0% under RCP8.5, respectively (Table 3). The coefficient of variation (CV) varied across the regions and scenarios, ranging from 2.4% to 12.7% in Kafer, from 2.8% to 11.3% in Orman, and from 3.2% to 12.7% in Ain Arab. Moreover, the study estimated that the highest decrease in HTC under RCP2.6 compared to the baseline was in Orman (−51.9%), followed by Kafer (−18.0%) and Ain Arab (−14.5%). This same trend was also observed under RCP4.5 and RCP8.5, with magnitudes of −71.2%, −47.4%, and −46.9% under RCP4.5, and −67.7%, −41.7%, and −38.3% under RCP8.5, respectively (Table 3 and Figure 4). The CV varied across the regions and scenarios, ranging from 28.7% to 64.2% in Orman, from 31.3% to 55.3% in Kafer, and from 27.0% to 58.8% in Ain Arab. Finally, the study estimated that the highest increase in CI under RCP2.6 compared to the baseline was in Orman (11.5%), followed by Kafer (9.4%) and Ain Arab (6.0%). The same trend was observed under RCP4.5, with values of 1.6%, 0.4%, and −3.9% in Orman, Kafer, and Ain Arab, respectively. Under RCP8.5, however, the highest increase was estimated in Ain Arab (39.1%), followed by Orman (22.2%) and Kafer (19.9%). The coefficient of variation (CV) varied from the lowest 2.8% under RCP2.6 to the highest 11.4% under RCP8.5, and 4.7% under RCP4.5 in Ain Arab, whereas in Kafer, the CV varied from 2.5% under RCP2.6 to the highest 9.0% under RCP8.5, and 4.0% under RCP4.5 and in Orman, the CV varied from the lowest 2.5% under RCP2.6 to the highest 9.1% under RCP8.5, and 4.3% under RCP4.5 (Table 3 and Figure 4).

Table 3. The percentage change in WI-GDD, HI, HTC, and CI for future scenarios spanning from 2015 to 2100 under RCP2.6, 4.5, and 8.5, in comparison to the baseline period of 1984–2014.

Regions	RCPs	WI-GDD	HI	HTC	CI
Ain Arab	RCP2.6	6.6	5.9	−14.5	6.0
	RCP4.5	16.1	15.8	−46.9	−3.9
	RCP8.5	22.9	21.0	−38.3	39.1
Kafer	RCP2.6	17.6	14.3	−18.0	9.4
	RCP4.5	28.0	22.5	−47.4	0.4
	RCP8.5	33.6	26.6	−41.7	19.9
Orman	RCP2.6	18.5	16.2	−51.9	11.5
	RCP4.5	29.5	25.9	−71.2	1.6
	RCP8.5	35.8	30.8	−67.7	22.2

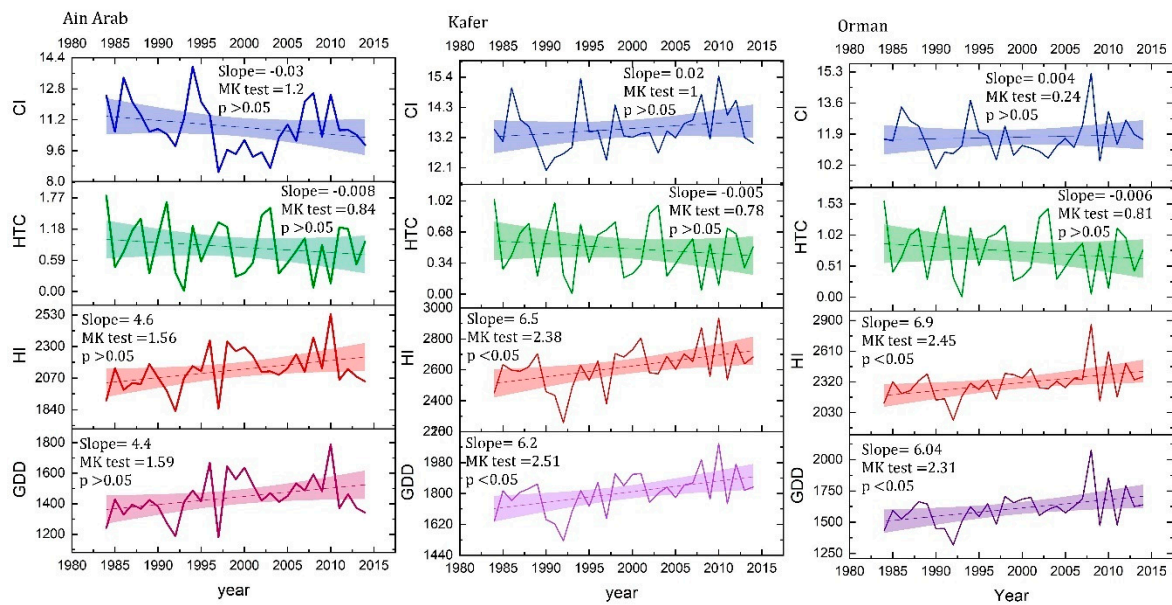


Figure 3. Temporal evolution of BVIs values during the 1984–2014 period for specific viticultural regions in the study area.

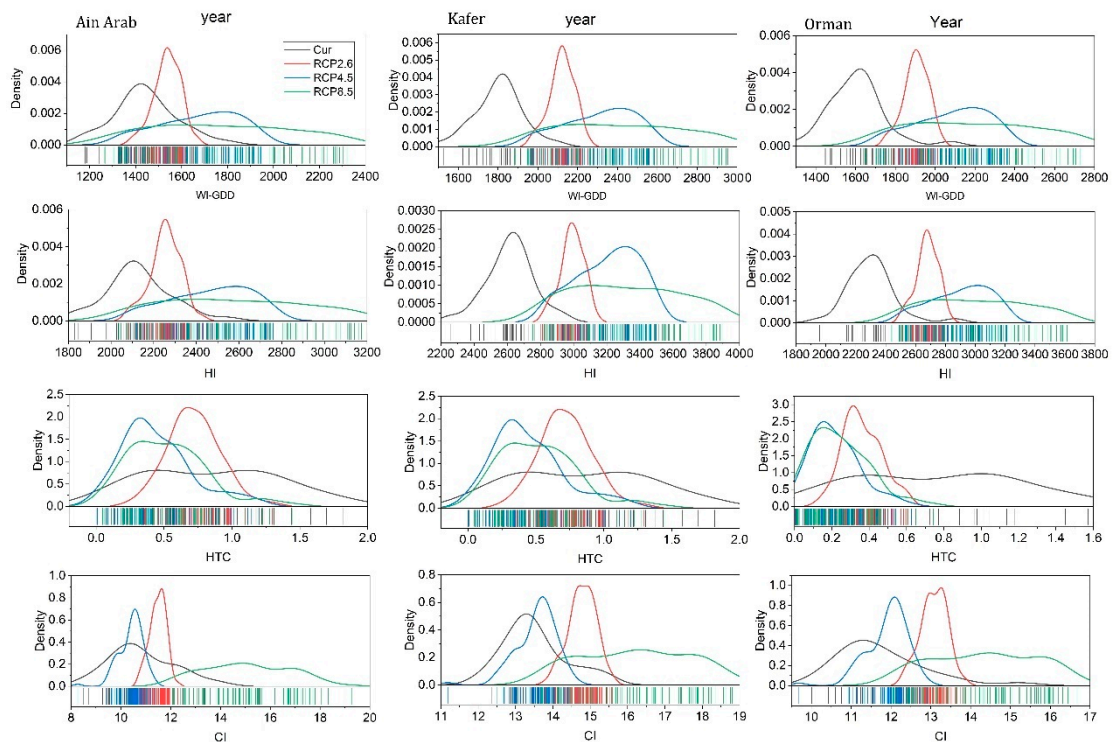


Figure 4. The kernel smoothed probability density function of the temporal distribution of BVIs values under projected climate change compared to the current climate for specific viticultural regions in the study area.

3.3. Delineation of BVIs Zones under Projected Climate Change

To assess the spatial distribution of BVIs zones at a 1 km spatial resolution, analyses were conducted using the RK method for both current climate conditions (referred to as the “1984–2014 period”) and projected climate change scenarios (RCPs). Zonal statistical analysis was performed for the study area, revealing significant changes between 1984 and 2014 and the RCPs (Figure 5). The results indicated that under current climate conditions,

the GST indicator showed that 71.7% of the study area was classified as the Hot zone (H), while the Warm (W) and Temperate (T) zones covered approximately 20% and 7.8% of the study area, respectively. However, when considering climate change scenarios, the Hot zone expanded significantly. It was projected that 91%, 96.5%, and 97.9% of the study area would be dominated by the Hot zone for the RCP2.6, RCP4.5, and RCP8.5 scenarios, respectively. These areas witnessed an increase of +20.3%, +24.8%, and +26.2% compared to the current climate conditions (see Table 4). Additionally, the Warm zone is expected to shift towards the elevated areas in the central part of the study area under climate change scenarios.

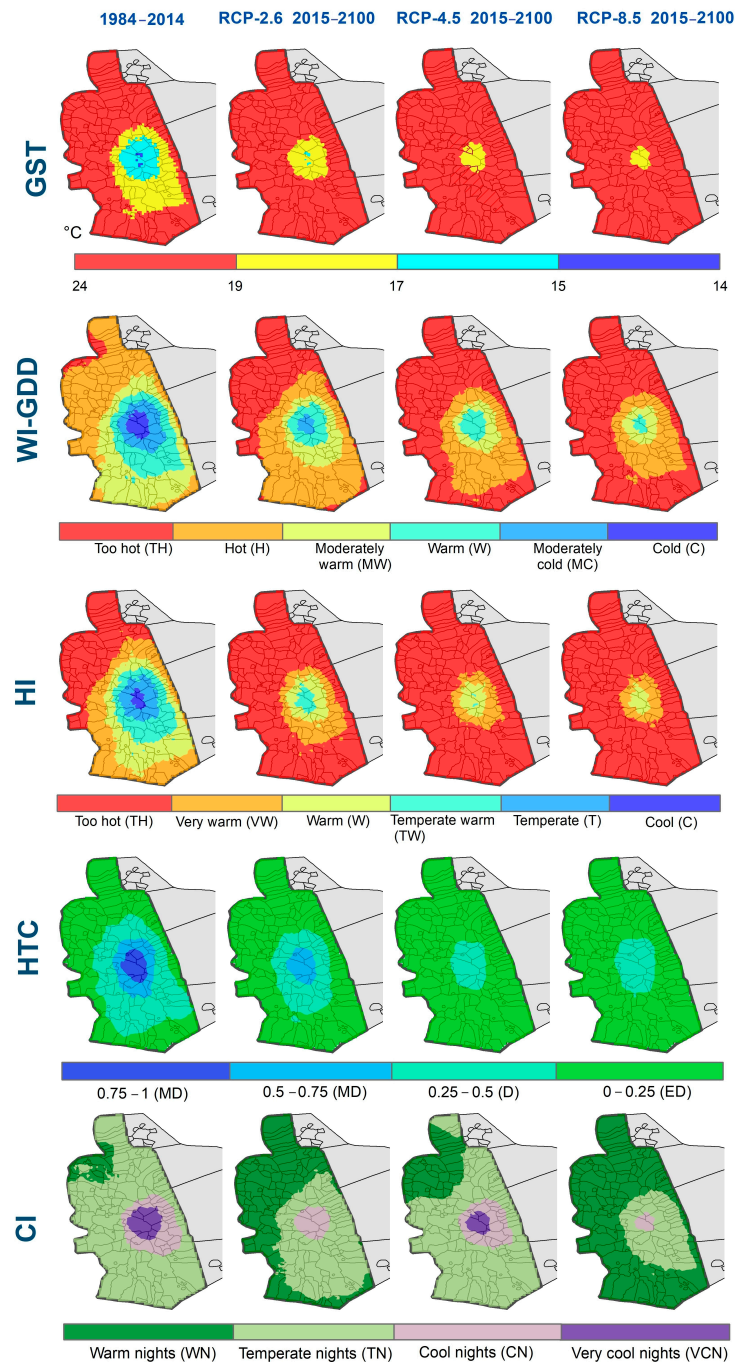


Figure 5. Spatial distribution of BVIs zones under current climate and projected climate change for three RCPs under sustainable development (RCP2.6), modest mitigation (RCP4.5), and unabated climate change (RCP8.5).

Table 4. Changes in percentage area (%) per zone of the BVI under projected climate change (2015–2100) and three RCPs compared to the current climate (1984–2014).

BVI	Zone	1984–2014	2015–2100		
			RCP2.6	RCP4.5	RCP8.5
GST	C	0.2	0 (−0.2)	0 (−0.2)	0 (−0.2)
	T	7.8	0.3 (−7.5)	0 (−7.8)	0 (−7.8)
	W	20.3	7.7	3.5	2.1
	H	71.7	92 (+20.3)	96.5 (+24.8)	97.9 (+26.2)
WI-GDD	C	2.9	0 (−2.9)	0 (−2.9)	0 (−2.9)
	MC	8	1.7 (−6.3)	0 (−8)	0 (−8)
	W	15.8	6.4 (−9.4)	3.8 (−12)	1.1 (−14.7)
	MW	30.3	11.8 (−18.5)	7 (−23.3)	5.2 (−25.1)
	H	40.3	43.6 (+3.3)	28.5 (−11.8)	21.2 (−19.1)
HI	TH	2.6	36.5 (+33.9)	60.7 (+58.1)	72.5 (+69.6)
	C	1.3	0 (−1.3)	0 (−1.3)	0 (−1.3)
	T	7.2	0 (−7.2)	0 (−7.2)	0 (−7.2)
	TW	13.3	2.3 (−11)	0.2 (−13.1)	0 (−13.3)
	W	21.3	7.2 (−14.1)	4.1 (−17.2)	2.5 (−18.8)
HTC	VW	26.5	13.8 (−12.7)	8.5 (−18)	7.3 (−19.2)
	TH	30.4	76.7 (+46.3)	87.2 (+56.8)	90.2 (+59.8)
	ED	52.8	75.5 (+22.7)	91.3 (+38.5)	88.9 (+36.1)
	D	34.9	19.6 (−15.3)	8.7 (−26.2)	11.1 (−23.8)
	MD	12.3	4.9 (−7.4)	0 (−12.3)	0 (−12.3)
CI	VCN	4.2	0 (−4.2)	2.2 (−2)	0 (−4.2)
	CN	6.7	3.1 (−3.6)	5.1 (−1.6)	1.7 (−5)
	TN	85.8	43.3 (−42.5)	77.1 (−8.7)	22.4 (−63.4)
	WN	3.3	53.6 (+50.3)	15.6 (+12.3)	75.9 (+72.6)

The values in parentheses are the percentage of change (%) compared to current climate values.

Since the WI-GDD and HI provide information on the accumulation of heat during the growing season for vineyards, and thus provide better information regarding the sugar potential accumulation of given varieties and climate-maturity zoning, we assessed the spatial distribution of WI-GDD and HI as given in Figure 5 for both current climate conditions and RCPs. The results indicated that under current climate conditions, the WI-GDD showed that only 2.6% of the study area was classified as the Too Hot zone (TH), while the Hot (H) zone covered approximately 40.3% of the study area. However, when considering climate change scenarios (RCPs), the Too Hot zone expanded significantly. It was projected that 36.5%, 60.7%, and 72.5% of the study area would be dominated by the Too Hot zone for the RCP2.6, RCP4.5, and RCP8.5 scenarios, respectively. These areas witnessed an increase of +33.9%, +58.1%, and +69.6% compared to the current climate conditions (see Table 4). Moreover, the Hot zone and Moderately Warm (MW) zone are expected to shift towards the elevated areas in the central part of the study area under climate change scenarios, resulting in a decrease in their percentage distribution compared to the current climate conditions. Notably, the Moderately Cold (MC) and Warm (W) zones, which are the most important zones for viticulture cultivation, are projected to decrease under climate change scenarios. The MC zone is expected to decrease by 6.3%, 8%, and 8% from the study area, while the W zone is expected to decrease by 9.4%, 3.8%, and 14.7% from the study area, for the RCP2.6, RCP4.5, and RCP8.5 scenarios, respectively, compared to the current climate. The same results were obtained for the HI zones with slight changes compared to the WI-GDD (see Figure 5 and Table 4).

In terms of the spatial distribution of HTC, which determines the suitability for rainfed viticulture, the study classified the region into six classes ranging from excessively dry

(ED) to excessively wet (EW) (Table 2). The results indicated that under current climate conditions, the study area can be divided into three zones: ED, D, and MD zones, covering approximately 52.8%, 34.9%, and 12.3% of the study area, respectively. The MD zone, considered the optimal region with HTC values ranging from 0.5 to 1.0 mm/°C, is expected to decrease by 7.4% in terms of coverage area under the RCP2.6 scenario. However, this zone is projected to disappear entirely under the RCP4.5 and RCP8.5 scenarios. These findings suggest that grape production based on these scenarios would only be possible with irrigation due to the unsuitability of the climate for rainfed viticulture.

In terms of the spatial distribution of CI, which is a significant indicator of grape and wine color and aromas, the study examined its variations under both current climate conditions and different RCPs scenarios. The findings revealed that the study area can be classified into four zones under current climate conditions: VCN, CN, TN, and WN zones, covering approximately 4.2%, 6.7%, 85.8%, and 3.3% of the study area, respectively. The WN zone is projected to expand by +50.3%, +12.3%, and +72.6% from the study area under the RCP2.6, RCP4.5, and RCP8.5 scenarios, respectively. On the other hand, the CN zone (considered the optimal region with CI values >12 and ≤14 C) is expected to decrease by 3.6%, 1.6%, and 5% from the study area under the RCP2.6, RCP4.5, and RCP8.5 scenarios. Furthermore, the VCN zone is anticipated to disappear under the RCP2.6 and RCP8.5 scenarios. These findings suggest that the warming projected under the RCPs will significantly impact the spatial distribution of CI, subsequently influencing the quality of grapes in terms of secondary metabolites such as aromas and polyphenols. It can also impede sugar accumulation and anthocyanins. For more details regarding the BVIs values and zones under projected climate change compared to the current climate for major viticultural regions in the study area see Table 5.

Table 5. Changes in mean BVIs values and zones under projected climate change compared to the current climate for major viticultural regions in the study area.

Scenario	Region	W-GDD		HI		HTC		CI	
		Mean	Zone	Mean	Zone	Mean	Zone	Mean	Zone
Baseline 1982–2014	Alkars	1826.9	W	2368.9	TW	0.46	D	14.6	TN
	Euyun	1784.4	W	2318.8	TW	0.475	D	14.4	TN
	Orman	1859.4	W	2408.6	W	0.375	D	14.7	TN
	Qanawat	1626.5	MC	2140.9	TW	0.702	MD	12.7	CN
	Mafeila	1809.5	W	2289.3	TW	0.605	MD	14.2	TN
	Mayamas	1493.3	MC	1999.6	T	0.73	MD	12.1	CN
	Kafer	1631.6	MC	2137.7	TW	0.626	MD	12.8	CN
	Sahwat Kh	1657.6	MC	2183.5	TW	0.573	MD	13.3	CN
	Hobran	1855.4	W	2413	W	0.45	D	14.5	TN
RCP26 2015–2100	Alkars	2206.3	MW	2947.6	VW	0.325	D	16.6	TN
	Euyun	2159	MW	2900.6	VW	0.331	D	16.4	TN
	Orman	2244	H	2997.1	VW	0.252	D	16.6	TN
	Qanawat	1995	MW	2693.1	W	0.50	MD	14.6	TN
	Mafeila	2191.4	MW	2843.7	VW	0.440	D	16.1	TN
	Mayamas	1852.6	W	2546.2	W	0.522	MD	14.1	TN
	Kafer	1989.5	MW	2694.8	W	0.452	D	14.9	TN
	Sahwat Kh	2023.2	MW	2754.2	VW	0.407	D	15.4	TN
Hobran	2242.2	H	2980.9	VW	0.324	D	16.6	TN	

Table 5. Cont.

Scenario	Region	W-GDD		HI		HTC		CI	
		Mean	Zone	Mean	Zone	Mean	Zone	Mean	Zone
RCP45 2015–2100	Alkars	2407.7	H	3142.2	TH	0.191	ED	15.4	TN
	Euyun	2361.4	H	3095.2	TH	0.195	ED	15.1	TN
	Orman	2448	H	3191.7	TH	0.142	ED	15.4	TN
	Qanawat	2166.7	MW	2884.8	VW	0.307	D	13.5	CN
	Mafeila	2382.6	H	3036.5	TH	0.278	D	15	TN
	Mayamas	2013	MW	2740.6	VW	0.331	D	12.9	CN
	Kafer	2163.1	MW	2887.5	VW	0.279	D	13.6	CN
	Sahwat Kh	2211.3	MW	2948.3	VW	0.250	D	14.1	TN
	Hobran	2434.1	H	3173.2	TH	0.195	ED	15.3	TN
RCP85 2015–2100	Alkars	2551.5	H	3223.6	TH	0.219	ED	17.8	TN
	Euyun	2506.6	H	3181.4	TH	0.223	ED	17.6	TN
	Orman	2596.5	H	3284.4	TH	0.162	ED	17.85	TN
	Qanawat	2320.7	H	2971.6	VW	0.352	D	15.7	TN
	Mafeila	2537.2	H	3123.1	TH	0.318	D	17.3	TN
	Mayamas	2168	MW	2823.2	VW	0.365	D	15.4	TN
	Kafer	2309.3	H	2964.4	VW	0.3123	D	16.2	TN
	Sahwat Kh	2360.3	H	3032.4	TH	0.278	D	16.7	TN
	Hobran	2577.6	H	3245.9	TH	0.220	ED	18	WN

4. Discussion

Global warming and climatic change are the most deliberated matters in the last few decades due to their environmental, biological, and socio-economic consequences [63]. Global warming is likely to have a significant impact on agriculture and crop production [64,65], and especially on viticultural production, because grapevines are extremely vulnerable to climate change and variability [30,32,66–68]. Climate has a significant impact on agricultural aptitude and grapevine production [2,69,70]. Climate variables (solar radiation, air temperature, relative humidity, and rainfall amounts) that have a greater influence on grape growing and *Vitis vinifera* grapevine production, as well as wine grape quality, have been extensively studied in the case of the grapevine in response to increasing global warming, and according to some works (e.g., Cardell et al. [71]; Sgubin et al. [72]), temperature is regarded as the most important climatic variable affecting grapevine growth [73]. Grapevine composition and quality, in particular, are affected by air temperature [74,75], as well as wine qualities [5,76]; very cold temperatures can cause ripening to be delayed or even prevented, and can impede the sugar accumulation and anthocyanins formation, resulting in wines with poor alcohol content and poorly developed taste profiles [5,70,77,78]. Too much temperature throughout the season, on the other hand, might cause grapes to mature early in the growing season, with increased sugar formation but low acidity, resulting in an imbalanced wine [79,80]. Moreover, temperature fluctuation effects on vineyards have been seen to modify the duration of phenological periods and growth seasons, the timing and severity of diseases, and pests, resulting in effects on the quality and quantity of grapes produced [2,81–86].

The BVIs provide valuable insights into the suitability of different grape varieties for specific regions. However, with climate change projections indicating shifts in temperature and precipitation patterns, it is crucial to examine how these changes might affect viticultural indices in the study area. The changing climate can lead to shifts in climatic zones,

impacting the suitability of different grape varieties in current regions. The climatic classification systems, such as the HI and WI-GDD, and CI use temperature thresholds to define grape-growing regions. As these temperatures-based indices change, the boundaries of climatic zones will be changed. For example, cool-climate regions may experience warmer temperatures, allowing the cultivation of grape varieties that were previously unsuitable (elevated areas in Jabal Arab). Conversely, some traditional warm-climate regions (Kafer, Hobran, and Orman) may face a decline in suitability for certain grape varieties due to increased heat stress. Previous studies have indicated a northward shift in suitable viticultural regions in Europe, and regions such as Germany, England, Poland, and parts of Scandinavia and some central parts of Europe have seen an expansion in their viticultural potential due to milder temperatures and longer growing seasons [71,87,88]. In contrast, the temperatures-based indices such as the WI-GDD show an upward trend under climate change in many southern European viticulture regions; higher BVIs values indicate an increase in the heat available for grape ripening and this trend has been observed in regions such as the Apulia region in Italy [31], Douro Valley in Portugal [28], Lake Neuchatel in Switzerland [89], and Santorini Island in Greece [32].

Our study suggests that a changing climate can lead to shifts in the BVIs zones in the study area to being warmer, and will experience an increase in the WI-GDD, HI, TGS, and CI, potentially leading to alterations in grape variety suitability. For instance, some traditional grape-growing regions (Kafer, Hobran, Mayamas, and Orman) may become too hot for certain grape varieties, necessitating the adoption of heat-tolerant cultivars or the modification of some viticulture practices to mitigate the effects of climate change [90]. Furthermore, the viticultural regions cannot be shifted suddenly because of climatic change for a variety of socio-economic issues [91–95], such as long-dated reestablishment times, market accessibility, labor availability, and others. As a result, the importance of coping with climate change in viticulture is founded on three critical factors: (1) the grapevines are planted for several decades, and new plantations may take 15–30 years to yield full outputs; thus, the cultivars chosen should be adapted to rising temperatures and decreasing precipitation; (2) regulations on production practices and varieties adapt slowly; and (3) the properties of its final product are not only the outcome of “terroir”, which describes the relationship between vineyards, pedology, the cultivation process, and climatic variables, but also an expression of cultural and socio-economic parameters [96,97]. Although viticultural can adapt to the short- to medium-term effects of climate change, genetic enhancement is required to give long-term sustainable solutions to these issues [98,99]. As a result, the shifting of high-quality varieties to suitable areas for their cultivation (i.e., by their shifting to higher elevations, more than 1400 m) is possible in the future (see recommended grapevine cultivars in Table 6 under RCP2.6).

Table 6. Recommended grapevine cultivars based on climate-maturity zoning under baseline climate and scenario of sustainable development (RCP2.6) for major viticultural regions in the study area according to Jones’ classification [59].

Baseline and Scenario	Region	TGS (°C)		Recommended Grapevine Cultivars Based on Climate-Maturity Zoning
		Range	Zone	
Baseline 1982–2014	Alkars	17.6–18.6	W	Cabernet Franc, Tempranillo, Dolcetto, Merlot, Viognier Syrah, and Table grapes
	Euyun	17.8–18.4	W	
	Mayamas	15.4–17	T	Pinot Noir, Chardonnay, Sauvignon Blanc, and Semillon
	Qanawat	14.9–19.8	T–W	
	Mafeila	16.2–19	T–W	Chardonnay, Sauvignon Blanc, Semillon, Cabernet Franc, Tempranillo, Dolcetto, and Merlot
	Kafer	16.2–18.4	T–W	
	Sahwat Kh	15.7–18	T–W	
	Orman	17.7–19.5	W–H	Cabernet Franc, Tempranillo, Dolcetto, Merlot, Viognier, Syrah, Cabernet Sauvignon, Sangiovese, Grenache Carignane, and Table grapes,
	Hobran	17.8–19.7	W–H	

Table 6. Cont.

Baseline and Scenario	Region	TGS (°C)		Recommended Grapevine Cultivars Based on Climate-Maturity Zoning
		Range	Zone	
RCP26 2015–2100	Alkars	19.6–20.6	H	Table grapes, Grenache, Carignane, Zinfandel, Nebbiolo, and Raisins
	Euyun	19.8–20.4	H	
	Orman	19.7–21.5	H	
	Hobran	19.8–21.6	H	
	Mayamas	17.4–19	W	Cabernet Franc, Tempranillo, Dolcetto, Merlot, Viognier Syrah, and Table grapes
	Mafeila	18.1–21.9	W–H	Cabernet Franc, Tempranillo, Dolcetto, Merlot, Viognier Syrah, Table grapes, Cabernet Sauvignon Sangiovese, Grenache, Carignane, and Table grapes
	Kafer	18.1–20.3	W–H	
	Sahwat Kh	17.7–20.1	W–H	
	Qanawat	16.9–21.8	W–H	

5. Conclusions

The objective of this research was to evaluate the climatic zones for viticulture in the Jabal Arab region located in the Eastern Mediterranean. The study employed the RK method along with five bioclimatic indices. Historical and future time-series data until the end of the 21st century were analyzed. The findings indicated a rise in temperature as a result of climate change, which was already evident when comparing the historical periods of 1984–2014. This temperature increase is projected to continue in future scenarios, with varying values ranging from 0.8 °C to 4.1 °C depending on the considered RCPs. The bioclimatic indices used in this study revealed that under the milder and more reliable RCP2.6 scenario, there will still be opportunities for cultivating quality vineyards, even in smaller elevated areas than the current cultivated ones. However, the RCP8.5 and RCP4.5 scenarios indicated increasing trends of BVIs by the end of the century in the Jabal Arab region. These results emphasize the importance of territories such as Jabal Arab, which have a historical suitability for viticulture, to make prompt decisions to address climate change. This can be achieved by adjusting technical and agronomical practices to maintain competitiveness in the global grape market, especially considering the emergence of new players from regions where vineyard relocation has already begun.

It should be noted that these results do not necessarily imply a significant decline in viticulture suitability in the study area in the medium and long-term future scenarios, as adaptive strategies can be implemented, which are already being undertaken by grapevine growers in the region. In light of this, several actions can be recommended to preserve the typicity of high-quality varieties in the region, based on current knowledge and previous studies conducted in the area, such as Alsafadi et al. [100]. Key strategies include clonal selection, appropriate rootstocks, and the cultivation of late-ripening local or carefully selected non-local varieties to delay phenology stages. Training systems and late pruning can also be beneficial in delaying phenology and reducing water deficit. It is crucial to carefully assess the necessity of irrigation considering its economic, environmental, and social implications. Additionally, increasing the soil's water-holding capacity, selecting drought-resistant rootstocks, and implementing genetic enhancement is essential for achieving long-term sustainability.

Author Contributions: Conceptualization, K.A.; methodology, K.A.; software, K.A.; formal analysis, K.A.; investigation, K.A.; data curation, K.A.; writing—original draft preparation, K.A. and A.K.S.; writing—review and editing, K.A., S.B., B.B., A.A. and A.K.S.; visualization, K.A.; supervision, S.B.; funding acquisition, A.A., B.B. and S.B. All authors have read and agreed to the published version of the manuscript.

Funding: This work was supported by the Researchers Supporting Project (grant number RSP2023R296), King Saud University, Riyadh, Saudi Arabia, and was also supported by the National Natural Science Foundation of China (grant numbers 41971340 and 41271410). We also acknowledge the funding by

the German Federal Ministry of Education and Research (BMBF) in the framework of the funding measure “Soil as a Sustainable Resource for the Bioeconomy— BonaRes”, project BonaRes (Module A): BonaRes Center for Soil Research, subproject “Sustainable Subsoil Management—Soil3” (Grant 031B0151A), and partially funded by the Deutsche Forschungsgemeinschaft (DFG, German Research Foundation) under Germany’s Excellence Strategy—EXC 2070—390732324.

Institutional Review Board Statement: Not applicable.

Informed Consent Statement: Not applicable.

Data Availability Statement: The data that support the findings of this study are available upon request.

Conflicts of Interest: The authors declare no conflict of interest.

References

1. Vivier, M.A.; Pretorius, I.S. Genetically Tailored Grapevines for the Wine Industry. *Trends Biotechnol.* **2002**, *20*, 472–478. [CrossRef]
2. Ponti, L.; Gutierrez, A.P.; Boggia, A.; Neteler, M. Analysis of Grape Production in the Face of Climate Change. *Climate* **2018**, *6*, 20. [CrossRef]
3. Alsafadi, K.; Mohammed, S.; Habib, H.; Kiwan, S.; Hennawi, S.; Sharaf, M. An Integration of Bioclimatic, Soil, and Topographic Indicators for Viticulture Suitability Using Multi-Criteria Evaluation: A Case Study in the Western Slopes of Jabal Al Arab—Syria. *Geocarto Int.* **2020**, *35*, 1466–1488. [CrossRef]
4. Huggett, J.M. Geology and Wine: A Review. In *Proceedings of the Geologists’ Association*; Elsevier: Amsterdam, The Netherlands, 2006; Volume 117.
5. Jackson, D.I.; Lombard, P.B. Environmental and Management Practices Affecting Grape Composition and Wine Quality—A Review. *Am. J. Enol. Vitic.* **1993**, *44*, 409–430. [CrossRef]
6. Cardoso, A.S.; Alonso, J.; Rodrigues, A.S.; Araújo-Paredes, C.; Mendes, S.; Valín, M.I. Agro-Ecological Terroir Units in the North West Iberian Peninsula Wine Regions. *Appl. Geogr.* **2019**, *107*, 51–62. [CrossRef]
7. OIV Guidelines for Vitiviniculture Zoning. Methodologies on a Soil and Climate Level. Resolution OIV-VITI 423-2012 REV1. (Izmir). 2012. Available online: <https://www.oiv.int/public/medias/400/viti-2012-1-en.pdf> (accessed on 25 June 2023).
8. Amerine, M.A.; Winkler, A.J. Composition and Quality of Musts and Wines of California Grapes. *Hilgardia* **1944**, *15*, 493–675. [CrossRef]
9. Huglin, P. Nouveau mode d’évaluation des possibilités héliothermiques d’un milieu viticole. *Comptes Rendus L’acad. D’agricul. Fr.* **1978**, *64*, 89–98.
10. Tonietto, J.; Carbonneau, A. A Multicriteria Climatic Classification System for Grape-Growing Regions Worldwide. *Agric. For. Meteorol.* **2004**, *124*, 81–97. [CrossRef]
11. Branas, J.; Bernon, G.; Levadoux, L. *Elements de Viticulture Generale*; Imp. Dehan: Bordeaux, France, 1946.
12. Cabré, F.; Nuñez, M. Impacts of Climate Change on Viticulture in Argentina. *Reg. Environ. Change* **2020**, *20*, 12. [CrossRef]
13. Cabré, M.F.; Quénol, H.; Nuñez, M. Regional Climate Change Scenarios Applied to Viticultural Zoning in Mendoza, Argentina. *Int. J. Biometeorol.* **2016**, *60*, 1325–1340. [CrossRef] [PubMed]
14. Hall, A.; Jones, G.V. Spatial Analysis of Climate in Winegrape-Growing Regions in Australia. *Aust. J. Grape Wine Res.* **2010**, *16*, 389–404. [CrossRef]
15. Jarvis, C.; Barlow, E.; Darbyshire, R.; Eckard, R.; Goodwin, I. Relationship between Viticultural Climatic Indices and Grape Maturity in Australia. *Int. J. Biometeorol.* **2017**, *61*, 1849–1862. [CrossRef]
16. Santos, J.; Malheiro, A.; Pinto, J.; Jones, G. Macroclimate and Viticultural Zoning in Europe: Observed Trends and Atmospheric Forcing. *Clim. Res.* **2012**, *51*, 89–103. [CrossRef]
17. Anderson, J.D.; Jones, G.V.; Tait, A.; Hall, A.; Trought, M.C.T. Analysis of Viticulture Region Climate Structure and Suitability in New Zealand. *OENO One* **2012**, *46*, 149. [CrossRef]
18. Omazić, B.; Telišman Prtenjak, M.; Prša, I.; Belušić Vozila, A.; Vučetić, V.; Karoglan, M.; Karoglan Kontić, J.; Prša, Ž.; Anić, M.; Šimon, S.; et al. Climate Change Impacts on Viticulture in Croatia: Viticultural Zoning and Future Potential. *Int. J. Clim.* **2020**, *40*, 5634–5655. [CrossRef]
19. Montes, C.; Perez-Quezada, J.F.; Peña-Neira, A.; Tonietto, J. Climatic Potential for Viticulture in Central Chile. *Aust. J. Grape Wine Res.* **2012**, *18*, 20–28. [CrossRef]
20. Jones, G.V.; Duff, A.A.; Hall, A.; Myers, J.W. Spatial Analysis of Climate in Winegrape Growing Regions in the Western United States. *Am. J. Enol. Vitic.* **2010**, *61*, 313–326. [CrossRef]
21. Gaál, M.; Moriondo, M.; Bindi, M. Modelling the Impact of Climate Change on the Hungarian Wine Regions Using Random Forest. *Appl. Ecol. Environ. Res.* **2012**, *10*, 121–140. [CrossRef]
22. Vukovic, A.; Vujadinovic, M.; Ruml, M.; Rankovic-Vasic, Z.; Przic, Z.; Beslic, Z.; Matijasevic, S.; Vujovic, D.; Todoc, S.; Markovic, N.; et al. Implementation of Climate Change Science in Viticulture Sustainable Development Planning in Serbia. *Web Conf.* **2018**, *50*, 01005. [CrossRef]

23. Patriche, C.V.; Irimia, L.M. Mapping the Impact of Recent Climate Change on Viticultural Potential in Romania. *Theor. Appl. Clim.* **2022**, *148*, 1035–1056. [[CrossRef](#)]
24. Jones, N.K. An Investigation of Trends in Viticultural Climatic Indices in Southern Quebec, a Cool Climate Wine Region. *J. Wine Res.* **2018**, *29*, 120–129. [[CrossRef](#)]
25. Badr, G.; Hoogenboom, G.; Abouali, M.; Moyer, M.; Keller, M. Analysis of Several Bioclimatic Indices for Viticultural Zoning in the Pacific Northwest. *Clim. Res.* **2018**, *76*, 203–223. [[CrossRef](#)]
26. Blanco-Ward, D.; García Queijeiro, J.M.; Jones, G.V. Spatial Climate Variability and Viticulture in the Miño River Valley of Spain. *Vitis—J. Grapevine Res.* **2007**, *46*, 63.
27. Köse, B. Phenology and Ripening of *Vitis Vinifera*, L. and *Vitis Labrusca*, L. Varieties in the Maritime Climate of Samsun in Turkey's Black Sea Region. *S. Afr. J. Enol. Vitic.* **2014**, *35*, 90–102. [[CrossRef](#)]
28. Blanco-Ward, D.; Ribeiro, A.; Barreales, D.; Castro, J.; Verdial, J.; Feliciano, M.; Viceto, C.; Rocha, A.; Carlos, C.; Silveira, C.; et al. Climate Change Potential Effects on Grapevine Bioclimatic Indices: A Case Study for the Portuguese Demarcated Douro Region (Portugal). *BIO Web Conf.* **2019**, *12*, 01013. [[CrossRef](#)]
29. Santos, J.A.; Malheiro, A.C.; Karremann, M.K.; Pinto, J.G. Statistical Modelling of Grapevine Yield in the Port Wine Region under Present and Future Climate Conditions. *Int. J. Biometeorol.* **2011**, *55*, 119–131. [[CrossRef](#)] [[PubMed](#)]
30. Alba, V.; Gentileco, G.; Tarricone, L. Climate Change in a Typical Apulian Region for Table Grape Production: Spatialisation of Bioclimatic Indices, Classification and Future Scenarios. *OENO One* **2021**, *55*, 317–336. [[CrossRef](#)]
31. Gentileco, G.; Coletta, A.; Tarricone, L.; Alba, V. Bioclimatic Characterization Relating to Temperature and Subsequent Future Scenarios of Vine Growing across the Apulia Region in Southern Italy. *Agriculture* **2023**, *13*, 644. [[CrossRef](#)]
32. Xyrafis, E.G.; Fraga, H.; Nakas, C.T.; Koundouras, S. A Study on the Effects of Climate Change on Viticulture on Santorini Island. *OENO One* **2022**, *56*, 259–273. [[CrossRef](#)]
33. Mohammed, S.; Alsafadi, K.; Talukdar, S.; Kiwan, S.; Hennawi, S.; Alshihabi, O.; Sharaf, M.; Harsanyie, E. Estimation of Soil Erosion Risk in Southern Part of Syria by Using RUSLE Integrating Geo Informatics Approach. *Remote Sens. Appl. Soc. Environ.* **2020**, *20*, 100375. [[CrossRef](#)]
34. Alsafadi, K.; Bi, S.; Abdo, H.G.; Almohamad, H.; Alatrach, B.; Srivastava, A.K.; Al-Mutiry, M.; Bal, S.K.; Chandran, M.A.S.; Mohammed, S. Modeling the Impacts of Projected Climate Change on Wheat Crop Suitability in Semi-Arid Regions Using the AHP-Based Weighted Climatic Suitability Index and CMIP6. *Geosci. Lett.* **2023**, *10*, 20. [[CrossRef](#)]
35. Mohammed, S.; Alsafadi, K.; Hennawi, S.; Mousavi, S.M.N.; Kamal-Eddin, F.B.; Harsanyie, E. Effects of Long-Term Agricultural Activities on the Availability of Heavy Metals in Syrian Soil: A Case Study in Southern Syria. *J. Saudi Soc. Agric. Sci.* **2021**, *20*, 497–505. [[CrossRef](#)]
36. Mohammed, S.; Alsafadi, K.; Enaruvbe, G.O.; Harsányi, E. Assessment of Soil Micronutrient Level for Vineyard Production in Southern Syria. *Model. Earth Syst. Environ.* **2021**, *8*, 407–416. [[CrossRef](#)]
37. Hall, A.; Blackman, J. Modelling Within-Region Spatiotemporal Variability in Grapevine Phenology with High Resolution Temperature Data. *Oeno One* **2019**, *53*, 147–159. [[CrossRef](#)]
38. Sturman, A.; Zavar-Reza, P.; Soltanzadeh, I.; Katurji, M.; Bonnardot, V.; Parker, A.K.; Trought, M.C.T.; Quéno, H.; Le Roux, R.; Gendig, E.; et al. The Application of High-Resolution Atmospheric Modelling to Weather and Climate Variability in Vineyard Regions. *OENO One* **2017**, *51*, 99. [[CrossRef](#)]
39. Le Roux, R.; de Ressaiguier, L.; Corpetti, T.; Jégou, N.; Madelin, M.; van Leeuwen, C.; Quéno, H. Comparison of Two Fine Scale Spatial Models for Mapping Temperatures inside Winegrowing Areas. *Agric. For. Meteorol.* **2017**, *247*, 159–169. [[CrossRef](#)]
40. Morari, F.; Castrignanò, A.; Pagliarin, C. Application of Multivariate Geostatistics in Delineating Management Zones within a Gravelly Vineyard Using Geo-Electrical Sensors. *Comput. Electron. Agric.* **2009**, *68*, 97–107. [[CrossRef](#)]
41. Blanco-Ward, D.; Monteiro, A.; Lopes, M.; Borrego, C.; Silveira, C.; Viceto, C.; Rocha, A.; Ribeiro, A.; Andrade, J.; Feliciano, M.; et al. Climate Change Impact on a Wine-Producing Region Using a Dynamical Downscaling Approach: Climate Parameters, Bioclimatic Indices and Extreme Indices. *Int. J. Clim.* **2019**, *39*, 5741–5760. [[CrossRef](#)]
42. Hofmann, M.; Volosciuk, C.; Dubrovský, M.; Maraun, D.; Schultz, H.R. Downscaling of Climate Change Scenarios for a High-Resolution, Site-Specific Assessment of Drought Stress Risk for Two Viticultural Regions with Heterogeneous Landscapes. *Earth Syst. Dyn.* **2022**, *13*, 911–934. [[CrossRef](#)]
43. Le Roux, R.; Katurji, M.M.; Zavar-Reza, P.; de Resseguier, L.; Sturman, A.P.; van Leeuwen, C.; Parker, A.; Trought, M.; Quenol, H. A fine scale approach to map bioclimatic indices using and comparing dynamical and geostatistical methods. In Proceedings of the 11th International Terroir Congress, Willamette Valley, OR, USA, 10–14 July 2016.
44. Zorer, R.; Rocchini, D.; Metz, M.; Delucchi, L.; Zotte, F.; Meggio, F.; Neteler, M. Daily MODIS Land Surface Temperature Data for the Analysis of the Heat Requirements of Grapevine Varieties. *IEEE Trans. Geosci. Remote Sens.* **2013**, *51*, 2128–2135. [[CrossRef](#)]
45. Morin, G.; Roux, R.; Lemasle, P.-G.; Quéno, H. Mapping Bioclimatic Indices by Downscaling Modis Land Surface Temperature: Case Study of the Saint-Emilion Area. *Remote Sens.* **2021**, *13*, 4. [[CrossRef](#)]
46. Moral, F.J.; Rebollo, F.J.; Paniagua, L.L.; García, A. Climatic Spatial Variability in Extremadura (Spain) Based on Viticultural Bioclimatic Indices. *Int. J. Biometeorol.* **2014**, *58*, 2139–2152. [[CrossRef](#)]
47. Alsafadi, K.; Mohammed, S.; Mokhtar, A.; Sharaf, M.; He, H. Fine-Resolution Precipitation Mapping over Syria Using Local Regression and Spatial Interpolation. *Atmos. Res.* **2021**, *256*, 105524. [[CrossRef](#)]

48. Alsafadi, K.; Bi, S.; Bashir, B.; Sharifi, E.; Alsalman, A.; Kumar, A.; Shahid, S. High-Resolution Precipitation Modeling in Complex Terrains Using Hybrid Interpolation Techniques: Incorporating Physiographic and MODIS Cloud Cover Influences. *Remote Sens.* **2023**, *15*, 2435. [[CrossRef](#)]
49. Alexandersson, H. A Homogeneity Test Applied to Precipitation Data. *J. Climatol.* **1986**, *6*, 661–675. [[CrossRef](#)]
50. Štěpánek, P.; Zahradníček, P.; Skalák, P. Data Quality Control and Homogenization of Air Temperature and Precipitation Series in the Area of the Czech Republic in the Period 1961–2007. *Adv. Sci. Res.* **2009**, *3*, 23–26. [[CrossRef](#)]
51. Wilby, R.L.; Dawson, C.W.; Barrow, E.M. SDSM—A Decision Support Tool for the Assessment of Regional Climate Change Impacts. *Environ. Model. Softw.* **2002**, *17*, 145–157. [[CrossRef](#)]
52. Tavakol-Davani, H.; Nasser, M.; Zahraie, B. Improved Statistical Downscaling of Daily Precipitation Using SDSM Platform and Data-Mining Methods. *Int. J. Clim.* **2013**, *33*, 2561–2578. [[CrossRef](#)]
53. Meenu, R.; Rehana, S.; Mujumdar, P.P. Assessment of Hydrologic Impacts of Climate Change in Tunga-Bhadra River Basin, India with HEC-HMS and SDSM. *Hydrol. Process.* **2013**, *27*, 1572–1589. [[CrossRef](#)]
54. Gebrechorkos, S.H.; Hülsmann, S.; Bernhofer, C. Statistically Downscaled Climate Dataset for East Africa. *Sci. Data* **2019**, *6*, 31. [[CrossRef](#)]
55. Mesterházy, I.; Mészáros, R.; Pongrácz, R. The Effects of Climate Change on Grape Production in Hungary. *Idojaras* **2014**, *118*, 193–206.
56. Jones, G.V.; Duff, A.A.; Hall, A. Updated analysis of climate-viticulture structure and suitability in the Western United States. In Proceedings of the 16th International GIESCO Symposium-Davis, Viticulture and Enology, Davis, CA, USA, 12–15 July 2009.
57. Kliewer, W.M. Berry Composition of *Vitis Vinifera* Cultivars as Influenced by Photo- and Nycto-Temperatures During Maturation. *J. Am. Soc. Hortic. Sci.* **1973**, *98*, 153–159. [[CrossRef](#)]
58. Fraga, H.; Malheiro, A.C.; Moutinho-Pereira, J.; Cardoso, R.M.; Soares, P.M.M.; Cancela, J.J.; Pinto, J.G.; Santos, J.A. Integrated Analysis of Climate, Soil, Topography and Vegetative Growth in Iberian Viticultural Regions. *PLoS ONE* **2014**, *9*, e108078. [[CrossRef](#)] [[PubMed](#)]
59. Jones, G.V. Climate and Terroir: Impacts of Climate Variability and Change on Win. In *Fine Wine and Terroir—The Geoscience Perspective*; Macqueen, R.W., Meinert, L.D., Eds.; Geoscience Canada Reprint Series Number 9; Geological Association of Canada: St. John's, NL, Canada, 2006; 247p.
60. Odeh, I.O.A.; McBratney, A.B.; Chittleborough, D.J. Further Results on Prediction of Soil Properties from Terrain Attributes: Heterotopic Cokriging and Regression-Kriging. *Geoderma* **1995**, *67*, 215–226. [[CrossRef](#)]
61. Hengl, T.; Heuvelink, G.B.M.; Rossiter, D.G. About Regression-Kriging: From Equations to Case Studies. *Comput. Geosci.* **2007**, *33*, 1301–1315. [[CrossRef](#)]
62. Danielson, J.J.; Gesch, D.B. *Global Multi-Resolution Terrain Elevation Data 2010 (GMTED2010)*; US Department of the Interior, US Geological Survey: Reston, VA, USA, 2011; p. 101.
63. IPCC. *Climate Change 2014: Synthesis Report. Contribution of Working Groups I, II and III to the Fifth Assessment Report of the Intergovernmental Panel on Climate Change*; IPCC: Geneva, Switzerland, 2014.
64. Mokhtar, A.; Elbeltagi, A.; Maroufpoor, S.; Azad, N.; He, H.; Alsafadi, K.; Gyasi-Agyei, Y.; He, W. Estimation of the Rice Water Footprint Based on Machine Learning Algorithms. *Comput. Electron. Agric.* **2021**, *191*, 106501. [[CrossRef](#)]
65. Mokhtar, A.; He, H.; Alsafadi, K.; Li, Y.; Zhao, H.; Keo, S.; Bai, C.; Abuarab, M.; Zhang, C.; Elbagoury, K.; et al. Evapotranspiration as a Response to Climate Variability and Ecosystem Changes in Southwest, China. *Environ. Earth Sci.* **2020**, *79*, 312. [[CrossRef](#)]
66. Fraga, H.; Pinto, J.G.; Santos, J.A. Climate Change Projections for Chilling and Heat Forcing Conditions in European Vineyards and Olive Orchards: A Multi-Model Assessment. *Clim. Change* **2019**, *152*, 179–193. [[CrossRef](#)]
67. Piña-Rey, A.; González-Fernández, E.; Fernández-González, M.; Lorenzo, M.N.; Rodríguez-Rajo, F.J. Climate Change Impacts Assessment on Wine-Growing Bioclimatic Transition Areas. *Agriculture* **2020**, *10*, 605. [[CrossRef](#)]
68. Petriashvili, A.; Mach, J.; Štěbeták, M.; Prášilová, M.; Svoboda, R.; Navrátilová, M.; Beranová, M.; Veselá, K.; Hofman, V.; Němec, O. The Impact of Climate Change on the Sustainability of Wine Production and the Structure of Its Consumption in Czechia. *Heliyon* **2023**, *9*, e17882. [[CrossRef](#)]
69. Ramos, M.C.; Jones, G.V.; Martínez-Casasnovas, J.A. Structure and Trends in Climate Parameters Affecting Winegrape Production in Northeast Spain. *Clim. Res.* **2008**, *38*, 1–15. [[CrossRef](#)]
70. Arias, L.A.; Berli, F.; Fontana, A.; Bottini, R.; Piccoli, P. Climate Change Effects on Grapevine Physiology and Biochemistry: Benefits and Challenges of High Altitude as an Adaptation Strategy. *Front. Plant Sci.* **2022**, *13*, 835425. [[CrossRef](#)] [[PubMed](#)]
71. Cardell, M.F.; Amengual, A.; Romero, R. Future Effects of Climate Change on the Suitability of Wine Grape Production across Europe. *Reg. Environ. Change* **2019**, *19*, 2299–2310. [[CrossRef](#)]
72. Sgubin, G.; Swingedouw, D.; Mignot, J.; Gambetta, G.A.; Bois, B.; Loukos, H.; Noël, T.; Pieri, P.; de Cortázar-Atauri, I.; Ollat, N.; et al. Non-Linear Loss of Suitable Wine Regions over Europe in Response to Increasing Global Warming. *Glob. Change Biol.* **2023**, *29*, 808–826. [[CrossRef](#)] [[PubMed](#)]
73. Jones, G.V. Climate, Grapes, and Wine: Structure and Suitability in a Changing Climate. In Proceedings of the Acta Horticulturae, Alnarp, Sweden, 31 May–3 June 2015; Volume 931.
74. Coombe, B.G. Distribution of Solutes within the Developing Grape Berry in Relation to Its Morphology. *Am. J. Enol. Vitic.* **1987**, *38*, 120–127. [[CrossRef](#)]

75. Van Leeuwen, C.; Tregoat, O.; Choné, X.; Bois, B.; Pernet, D.; Gaudillière, J.P. Vine Water Status Is a Key Factor in Grape Ripening and Vintage Quality for Red Bordeaux Wine. How Can It Be Assessed for Vineyard Management Purposes? *Oeno One* **2009**, *43*, 121–134. [[CrossRef](#)]
76. Jones, G.V.; White, M.A.; Cooper, O.R.; Storchmann, K. Climate Change and Global Wine Quality. *Clim. Change* **2005**, *73*, 319–343. [[CrossRef](#)]
77. Sadras, V.O.; Moran, M.A. Elevated Temperature Decouples Anthocyanins and Sugars in Berries of Shiraz and Cabernet Franc. *Aust. J. Grape Wine Res.* **2012**, *18*, 115–122. [[CrossRef](#)]
78. Clemente, N.; Santos, J.A.; Fontes, N.; Graça, A.; Gonçalves, I.; Fraga, H. Grapevine Sugar Concentration Model (GSCM): A Decision Support Tool for the Douro Superior Winemaking Region. *Agronomy* **2022**, *12*, 1404. [[CrossRef](#)]
79. Mira de Orduña, R. Climate Change Associated Effects on Grape and Wine Quality and Production. *Food Res. Int.* **2010**, *43*, 1844–1855. [[CrossRef](#)]
80. Lakatos, L.; Mitre, Z. Effect of Drought on the Future Sugar Content of Wine Grape Varieties till 2100: Possible Adaptation in the Hungarian Eger Wine Region. *Biomolecules* **2023**, *13*, 1143. [[CrossRef](#)] [[PubMed](#)]
81. Valori, R.; Costa, C.; Figorilli, S.; Ortenzi, L.; Manganiello, R.; Ciccioritti, R.; Cecchini, F.; Morassut, M.; Bevilacqua, N.; Colatosti, G.; et al. Advanced Forecasting Modeling to Early Predict Powdery Mildew First Appearance in Different Vines Cultivars. *Sustainability* **2023**, *15*, 2837. [[CrossRef](#)]
82. Ausseil, A.G.E.; Law, R.M.; Parker, A.K.; Teixeira, E.I.; Sood, A. Projected Wine Grape Cultivar Shifts Due to Climate Change in New Zealand. *Front. Plant Sci.* **2021**, *12*, 618039. [[CrossRef](#)]
83. Costa, R.; Fraga, H.; Fonseca, A.; De Cortázar-Atauri, I.G.; Val, M.C.; Carlos, C.; Reis, S.; Santos, J.A. Grapevine Phenology of Cv. Touriga Franca and Touriga Nacional in the Douro Wine Region: Modelling and Climate Change Projections. *Agronomy* **2019**, *9*, 210. [[CrossRef](#)]
84. Verdugo-Vásquez, N.; Acevedo-Opazo, C.; Valdés-Gómez, H.; Araya-Alman, M.; Ingram, B.; García de Cortázar-Atauri, I.; Tisseyre, B. Spatial Variability of Phenology in Two Irrigated Grapevine Cultivar Growing under Semi-Arid Conditions. *Precis. Agric.* **2016**, *17*, 218–245. [[CrossRef](#)]
85. Sadras, V.O.; Moran, M.A. Nonlinear Effects of Elevated Temperature on Grapevine Phenology. *Agric. For. Meteorol.* **2013**, *173*, 107–115. [[CrossRef](#)]
86. Caffarra, A.; Rinaldi, M.; Eccel, E.; Rossi, V.; Pertot, I. Modelling the Impact of Climate Change on the Interaction between Grapevine and Its Pests and Pathogens: European Grapevine Moth and Powdery Mildew. *Agric. Ecosyst. Environ.* **2012**, *148*, 89–101. [[CrossRef](#)]
87. Droulia, F.; Charalampopoulos, I. A Review on the Observed Climate Change in Europe and Its Impacts on Viticulture. *Atmosphere* **2022**, *13*, 837. [[CrossRef](#)]
88. Nesbitt, A.; Kemp, B.; Steele, C.; Lovett, A.; Dorling, S. Impact of Recent Climate Change and Weather Variability on the Viability of UK Viticulture—Combining Weather and Climate Records with Producers’ Perspectives. *Aust. J. Grape Wine Res.* **2016**, *22*, 324–335. [[CrossRef](#)]
89. Comte, V.; Schneider, L.; Calanca, P.; Rebetez, M. Effects of Climate Change on Bioclimatic Indices in Vineyards along Lake Neuchâtel, Switzerland. *Theor. Appl. Clim.* **2022**, *147*, 423–436. [[CrossRef](#)]
90. Cataldo, E.C.; Salvi, L.S.; Paoli, F.P.; Fucile, M.F.; Masciandaro, G.M.; Manzi, D.M.; Masini, C.M.M.; Mattii, G.B.M. Effects of Natural Clinoptilolite on Physiology, Water Stress, Sugar, and Anthocyanin Content in Sanforte (*Vitis vinifera* L.) Young Vineyard. *J. Agric. Sci.* **2021**, *159*, 488–499. [[CrossRef](#)]
91. Mosedale, J.R.; Abernethy, K.E.; Smart, R.E.; Wilson, R.J.; Maclean, I.M.D. Climate Change Impacts and Adaptive Strategies: Lessons from the Grapevine. *Glob. Change Biol.* **2016**, *22*, 3814–3828. [[CrossRef](#)] [[PubMed](#)]
92. Bernetti, I.; Menghini, S.; Marinelli, N.; Sacchelli, S.; Sottini, V.A. Assessment of Climate Change Impact on Viticulture: Economic Evaluations and Adaptation Strategies Analysis for the Tuscan Wine Sector. *Wine Econ. Policy* **2012**, *1*, 73–86. [[CrossRef](#)]
93. Santos, J.A.; Fraga, H.; Malheiro, A.C.; Moutinho-Pereira, J.; Dinis, L.-T.; Correia, C.; Moriondo, M.; Leolini, L.; Dibari, C.; Costafreda-Aumedes, S.; et al. A Review of the Potential Climate Change Impacts and Adaptation Options for European Viticulture. *Appl. Sci.* **2020**, *10*, 3092. [[CrossRef](#)]
94. Lereboullet, A.L.; Beltrando, G.; Bardsley, D.K. Socio-ecological adaptation to climate change: A comparative case study from the Mediterranean wine industry in France and Australia. *Agric. Ecosyst. Environ.* **2013**, *164*, 273–285. [[CrossRef](#)]
95. Battaglini, A.; Barbeau, G.; Bindi, M.; Badeck, F.W. European winegrowers’ perceptions of climate change impact and options for adaptation. *Reg. Environ. Change* **2009**, *9*, 61–73. [[CrossRef](#)]
96. Resco, P.; Iglesias, A.; Bardaji, I.; Sotés, V. Exploring Adaptation Choices for Grapevine Regions in Spain. *Reg. Environ. Change* **2016**, *16*, 979–993. [[CrossRef](#)]
97. Salvi, L.; Brunetti, C.; Cataldo, E.; Storchi, P.; Mattii, G.B. Eco-Physiological Traits and Phenylpropanoid Profiling on Potted *Vitis vinifera* L. cv Pinot Noir Subjected to Ascophyllum nodosum Treatments under Post-Veraison Low Water Availability. *Appl. Sci.* **2020**, *10*, 4473. [[CrossRef](#)]
98. Van Leeuwen, C.; Destrac-Irvine, A.; Dubernet, M.; Duchêne, E.; Gowdy, M.; Marguerit, E.; Pieri, P.; Parker, A.; De Ressaiguier, L.; Ollat, N. An Update on the Impact of Climate Change in Viticulture and Potential Adaptations. *Agronomy* **2019**, *9*, 514. [[CrossRef](#)]

99. Delrot, S.; Grimplet, J.; Carbonell-Bejerano, P.; Schwandner, A.; Bert, P.F.; Bavaresco, L.; Costa, L.D.; Di Gaspero, G.; Duchêne, E.; Hausmann, L.; et al. Genetic and Genomic Approaches for Adaptation of Grapevine to Climate Change. In *Genomic Designing of Climate-Smart Fruit Crops*; Springer: Berlin/Heidelberg, Germany, 2020.
100. Alsafadi, K.J. Climate and Its Impact on Cultivation of Apple and Grapes Crops in Alswuydaa Governorate-Syria. Unpublished Master's Thesis, Alexandria University, Alexandria, Egypt, 2016. (In Arabic)

Disclaimer/Publisher's Note: The statements, opinions and data contained in all publications are solely those of the individual author(s) and contributor(s) and not of MDPI and/or the editor(s). MDPI and/or the editor(s) disclaim responsibility for any injury to people or property resulting from any ideas, methods, instructions or products referred to in the content.